THE UNIVERSITY OF MICHIGAN

COLLEGE OF LITERATURE, SCIENCE, AND THE ARTS
Department of Physics

Technical Report No. 27

POLARIZATION PARAMETER IN ELASTIC PROTON-PROTON SCATTERING FROM 0.75 TO 2.84 GeV

Homer A. Neal
Michael J. Longo

ORA Project 03106

under contract with:

DEPARTMENT OF THE NAVY
OFFICE OF NAVAL RESEARCH
WASHINGTON, D.C.

CONTRACT NO. Nonr-1224(23)
NR-022-274

administered through:

OFFICE OF RESEARCH ADMINISTRATION ANN ARBOR

March 1967

This report was prepared as a paper for submission to The Physical Review.

TABLE OF CONTENTS

	Page
ABSTRACT	1
I. INTRODUCTION	2
II. THEORY	3
A. General Relations	3
B. Predictions of Regge Theory	5
III. EXPERIMENTAL TECHNIQUE	6
A. General Discussion	6
B. Beam Layout and Characteristics	8
C. Apparatus and Detection Logic	9
IV. ANALYSIS AND RESULTS	11
A. Data Corrections	11
B. Errors	13
C. Results	16
V. DISCUSSION	18
ACKNOWLEDGMENTS	21
REFERENCES	22
FOOTNOTES	24
FIGURE CAPTIONS	30

Polarization Parameter in Elastic Proton-Proton Scattering from 0.75 to 2.84 GeV*

Homer A. Neal** and Michael J. Longo
The University of Michigan, Ann Arbor, Michigan

ABSTRACT

The polarization parameter in elastic proton-proton scattering has been measured at 0.75, 1.03, 1.32, 1.63, 2.24, and 2.84 GeV by employing a double-scattering technique. An external proton beam from the Brookhaven Cosmotron was focused on a three-inch long liquid hydrogen target and the elastic recoil and scattered protons were detected in coincidence by scintillation counters. The polarization of the recoil beam was determined from the azimuthal asymmetry exhibited in its scattering from a carbon target. This asymmetry was measured by a pair of scintillation counter telescopes which symmetrically viewed the carbon target. The analyzing power of this system was previously determined in an independent calibration experiment employing a 40% polarized proton beam at the Carnegie Institute of Technology synchro-cyclotron. False asymmetries were cancelled to a high order by periodically rotating the analyzer 180° about the recoil beam line. Spark chambers were utilized to obtain the spatial distribution of the beam as it entered the analyzer; this information allowed an accurate determination of the corrections necessary to compensate for any misalignment of the axis of the analyzer relative to the incident beam centroid. Values of the polarization parameter as a function of the center-of-mass scattering angle are given for each incident beam energy. The predictions of the Regge theory for polarization in elastic proton-proton scattering and recently published phase shift solutions are compared with the experimental results. Surprisingly good agreement with the Regge predictions is found despite the low energies involved.

Polarization Parameter in Elastic Proton-Proton Scattering from 0.75 to 2.84 GeV*

Homer A. Neal** and Michael J. Longo
The University of Michigan, Ann Arbor, Michigan

I. INTRODUCTION

We have measured the polarization parameter in elastic proton-proton scattering at 0.75, 1.03, 1.32, 1.63, 2.24, and 2.84 GeV in a double-scattering experiment performed at the Brookhaven Cosmotron. While the differential scattering cross-section for elastic p-p collisions is well-known in the region 1 to 3 GeV, there was until recently a marked scarcity of corresponding polarization measurements. In this region, polarization data have been reported by Grannis, et al.,[1] at 1.7 and 2.85 GeV, by Bareyre, et al.,[2] at 1.7 GeV, and by Ducros, et al.,[3] at 1.03 and 1.19 GeV; however, the results of the two experiments at 1.7 GeV appear to be inconsistent. Preliminary results of the present experiment were reported in an earlier paper by the present authors.[4]

In general the central goal in the study of the proton-proton system is the construction of the complete scattering matrix for proton-proton collisions. The measurement of the necessary number of independent spin correlation parameters to unambiguously determine the scattering matrix is currently experimentally prohibitive. However, cross-section and polarization data alone

can impose stringent conditions on any theoretically predicted phase shifts. On the other hand, cross-section and polarization data can be used in conjunction with physical models to predict the possible phase shift solutions. The latter approach has been employed by Hama, who used one-boson and one-pion exchange models to obtain phase shift solutions for the proton-proton system at 1.7 and 2.85 GeV.[5] His results will be discussed in the light of our measurements.

In Section II we will recall the relationship between the polarization parameter and the coefficients of the spin scattering matrix and give the predictions of Regge pole theory for polarization in elastic proton-proton scattering. In Section III the experimental techniques will be described. The method of analysis, discussion of errors, and the results are presented in Section IV. Section V is devoted to the discussion of the results, particularly with regard to the predictions of the Regge theory and the phase shifts calculated by Hama.[5]

II. THEORY

A. General Relations

The polarization parameter in elastic proton-proton scattering is defined as the expectation value of the spin vector ($\vec{\sigma}$) of the scattered proton when the expectation value of the spin vector for the incident and target proton is zero. In terms of the density matrix formalism the polarization parameter can be expressed as

$$\vec{P} = \mathrm{Tr}(M\rho M^{+}\vec{\sigma})/\mathrm{Tr}(M\rho M^{+})$$

where ρ is the density matrix characterizing the initial unpolarized state and M is the spin space scattering matrix. It has been shown by Wolfenstein and Ashkin[6] that the most general form for the matrix M consistent with invariance under time reversal, particle exchange, and parity transformations is

$$M(\vec{K},\vec{K}') = BS + C(\vec{\sigma}_1 + \vec{\sigma}_2)\cdot\vec{n} + \{N(\vec{\sigma}_1\cdot\vec{n})(\vec{\sigma}_2\cdot\vec{n}) + \frac{1}{2}G[(\vec{\sigma}_1\cdot\vec{r})(\vec{\sigma}_2\cdot\vec{r}) + (\vec{\sigma}_1\cdot\vec{p})(\vec{\sigma}_2\cdot\vec{p})] + \frac{1}{2}H[(\vec{\sigma}_1\cdot\vec{r})(\vec{\sigma}_2\cdot\vec{r}) - (\vec{\sigma}_1\cdot\vec{p})(\vec{\sigma}_2\cdot\vec{p})]\}T ,$$

where $\vec{K}$ and $\vec{K}'$ are the incident and outgoing proton momenta in the center-of-mass system, B, C, N, G, H are functions of $\vec{K}\cdot\vec{K}'$ and $|\vec{K}|$, $\vec{\sigma}_\ell$ is the Pauli spin vector for particle ℓ, and

$$\vec{n} = \frac{\vec{K}\times\vec{K}'}{|\vec{K}\times\vec{K}'|} , \quad \vec{r} = \frac{\vec{K}-\vec{K}'}{|\vec{K}-\vec{K}'|} , \quad \vec{p} = \frac{\vec{K}+\vec{K}'}{|\vec{K}+\vec{K}'|} .$$

S and T are the singlet and triplet projection operators.

The coefficients in the above expression are related to the unpolarized differential cross section, I, and the polarization $P(\vec{P} = P\vec{n})$ by

$$I = \frac{1}{4}[\,|B|^2 + 8|C|^2 + |G-N|^2 + 2|N|^2 + 2|H|^2]$$

$$PI = 2\,\mathrm{Re}(C^{*}N).$$

Thus, a measurement of the polarization and cross section can give some information on the contribution of the C and N terms to the spin scattering matrix. The polarization can easily be related to phase shifts by substituting in the

above formulae the phase shift expansions for the coefficients B, C, N, G, H given by Wright.[7]

B. Predictions of Regge Theory

The hypothesis of Regge poles in high energy nucleon-nucleon scattering leads to relatively simple predictions for the polarization parameter in proton-proton scattering when certain assumptions are made. Expressions have been developed by Hara[8] and Muzinich[9] using the helicity formalism defined in the work of Jacob and Wick[10] and Goldberger, et al.[11]

The cross section for the process

$$p_{\lambda_1} + p_{\lambda_2} \rightarrow p_{\lambda_1'} + p_{\lambda_2'} ,$$

where λ refers to the proton helicity, can be expressed as

$$\frac{d\sigma}{d\Omega} = \frac{2\pi}{E} \left| \langle \lambda_1 \lambda_2 | M | \lambda_1' \lambda_2' \rangle \right|^2 ,$$

where E is the total energy in the center-of-mass system, and M is the scattering matrix. Following Goldberger, et al.,[11] if we define

$$M_1 = \langle ++ | M | ++ \rangle$$

$$M_2 = \langle ++ | M | -- \rangle$$

$$M_3 = \langle +- | M | +- \rangle$$

$$M_4 = \langle +- | M | -+ \rangle$$

$$M_5 = \langle ++ | M | +- \rangle ,$$

the polarization parameter can be expressed as

$$P = \frac{\mathrm{Im}\{(M_1+M_2+M_3-M_4)M_5^*\}}{\frac{1}{2}\{|M_1|^2+|M_2|^2+|M_3|^2+|M_4|^2+4|M_5|^2\}} .$$

In the work of Hara and Muzinich the helicity amplitudes are Reggeized and lead to expressions for the polarization in terms of an expansion in Regge poles. Hara's resulting expression predicts a relation between the total cross sections for p-p and $\bar{p}$-p scattering and the p-p polarization parameter. The relations are

$$P(s,t) = \frac{\sigma(\bar{p}p)-\sigma(pp)}{\sigma(pp)} f(t) \qquad \text{(Ref. 8)}$$

$$P(s,t) = g(t)(s/s_o)^{h(t)} \qquad \text{(Ref. 9)},$$

where f, g and h are functions of the 4-momentum transfer squared, t, and s is the usual energy variable, with $s_o = 2m_p^2$.

These predictions will be compared with the experimental results in Section V.

III. EXPERIMENTAL TECHNIQUE

A. General Discussion

The polarization parameter was measured in the energy range 0.75 to 2.84 GeV by a double-scattering technique in which the polarization of the recoil proton beam was determined from the left-right azimuthal asymmetry exhibited in its scattering from a carbon target. The asymmetry was measured by a set

of two scintillation counter telescopes which symmetrically viewed the carbon target (Fig. 1). The analyzer was previously calibrated in an independent experiment employing a 40% polarized proton beam at the Carnegie Institute of Technology synchro-cyclotron for the range of energies 105 to 415 MeV, which encompassed most of the range of recoil energies analyzed in the primary experiment. The calibration was later extended to 1000 MeV by utilizing the antisymmetry of the polarization parameter about 90° in the center-of-mass system. At a given incident beam energy, the measurement of the polarization at center-of-mass angle θ_{cm} and the asymmetry parameter at angle $(\pi-\theta_{cm})$ is sufficient to determine the analyzing power at the recoil energy corresponding to the angle $(\pi-\theta_{cm})$. In the calibration experiment the correction to the measured analyzing power for any misalignment of the axis of the analyzer relative to the centroid of the incident beam was made by the utilization of spark chambers to sample the spatial distribution of the incident beam. Spark chambers were also employed in the primary experiment to allow any necessary corrections to the measured asymmetry due to possible misalignment of the analyzer axis relative to the recoil beam centroid. In order to cancel instrumental asymmetries the telescopes of the analyzer were periodically interchanged. Also, in order to insure that the incident proton beam was unpolarized, the recoil proton asymmetry was measured for several corresponding positive and negative scattering angles at each of the incident beam energies.

B. Beam Layout and Characteristics

The polarization measurements were made in an external proton beam at the Cosmotron. The beam optics employed is shown in Fig. 2. Because the virtual beam source in the Cosmotron moves laterally with energy, a small magnet, M300, was employed to make necessary angular corrections on the emerging beam. Two quadrupoles Q302 and Q303, then formed an intermediate focus between the two bending magnets, M304 and M305. The last pair of quadrupoles, Q306 and Q307, produced a second focus at the hydrogen target. The angular spread of the beam at the hydrogen target was approximately $\pm 0.5°$ and the diameter of the beam spot varied from $\approx 3/16$ in. at 2.84 GeV to $\approx 1\text{-}1/4$ in. at 0.75 GeV. The momentum spread was $\approx \pm 1.5\%$ at each energy, and the central value was known to $\pm 1.5\%$.

The incident beam intensity used was nominally 4×10^9 protons per pulse. At this level, all important accidental coincidence rates were consistently lower than 2%. The length of the beam spill was approximately 150 msec (with a duty cycle of $\approx 50\%$ within the spill).

Two pairs of scintillation counters, R_1-L_1 and R_2-L_2 (see Fig. 1) were employed in the tails of the incident beam to monitor the beam position and angle at all times. Also, a television camera was used to constantly view a 0.005 in. thick scintillator screen that was centered in the beam near the final focus. To reduce the background associated with protons in the halo of the incident beam at the final focus, a 24-in. deep, lead collimator with a 2-in. square aperture was placed just upstream of the hydrogen target.

The effect of background events due to scattering from the hydrogen target assembly was periodically investigated by counting with the target empty. In all cases the effect was entirely negligible.

C. Apparatus and Detection Logic

Plastic scintillation counters, viewed by RCA 6810-A photomultipliers through lucite light pipes, were employed to select and analyze protons elastically scattered from the 3-in. long liquid hydrogen target. In a typical analyzed event (Fig. 1) an elastic proton-proton scattering at the desired angle produces a count in S_1S_1' and $S_0(S_2$ or $S_2')$ with the appropriate time-of-flight difference. The recoil proton can then scatter from the analyzing target (carbon) into one of the telescopes T_1T_2 or U_1U_2. Anti-counter A_0 serves to greatly reduce the accidental rates by negating any chance coincidence that occurs when the proton scatters through too small an angle to be accepted by the telescopes. Anti-counters A_1 and A_2 serve primarily to reduce accidental events in which a proton directly enters one of the telescopes without passing through S_2 or S_2'.

The azimuthal asymmetry, ϵ, exhibited by the recoil beam in scattering from the carbon target is related to the polarization, P, by the well-known relation

$$\epsilon = PA$$

where A is the analyzing power. The quantity ϵ is just the fractional difference in events of the type MU_1U_2 and MT_1T_2, where $M \equiv S_1S_1'S_0(S_2$ or $S_2')$ $\bar{A}_0\bar{A}_1\bar{A}_2$. Specifically,

$$\epsilon = \pm \frac{MU_1U_2 - MT_1T_2}{MU_1U_2 + MT_1T_2}$$

where the sign is chosen according to the orientation of the telescope carriage. The telescopes were frequently interchanged to minimize the effect of instrumental asymmetries by rotating the telescope carriage 180° about the recoil beam line. A block diagram of the electronics is shown in Fig. 3.

Two thin plate spark chambers were employed just upstream of the analyzer and were triggered by each N^{th} successive analyzed proton, where N was typically set in the range 10 to 20. The camera which viewed the spark chambers also viewed two fiducial strips which rotated with the telescope carriage. Thus, in the analysis of the spark chamber data it was possible to correlate the space vector of each sampled event with the vector representing the axis of the analyzer.

Both the analyzer and the S_1-S_1' arm were mounted on tracks to facilitate the changing of angles. The S_1-S_1' counter sizes were varied to provide a fairly good match in the solid angles subtended by the two arms. Considerable care was taken in setting up at each angular position to insure that the centroid of the recoil proton beam was aligned with the axis of the analyzer. The two arms were first put at the proper angles by using a transit placed directly underneath the hydrogen target. If necessary the position of the S_1-S_1' arm was then adjusted to equalize the rates in the two halves of the S_2-S_2' counter.

Checks on possible contamination of the sample by protons (or pions) from inelastic events were made occasionally by moving the S_1-S_1' arm away from the correct kinematic angle for elastic events so that only inelastic events were

detected. The contamination was found to be negligible even at the highest 4-momentum transfers studied.

The amount of carbon in the analyzing target was changed with the recoil proton energy. For a particular recoil energy, the maximum thickness of the target was limited by the requirement that the protons, after the second scatter, have sufficient energy to be efficiently detected by the telescopes T and U. For high energy recoil protons it was possible to use more carbon, and the analyzing rates were therefore approximately constant over the center-of-mass angular range 20-80°. At the higher recoil energies, lead absorber was used between counters T_1 and T_2 (and U_1U_2) to discriminate against low energy background. Between 0.5% and 3% of the recoil protons which entered the analyzer scattered into the telescopes T and U. For a typical incident beam pulse of 4×10^9 protons, approximately 20 recoil protons scattered into the telescopes, and one spark chamber picture was taken.

Further details of the apparatus are described in an earlier report.[12]

IV. ANALYSIS AND RESULTS

A. Data Corrections

In the calibration experiment at the Carnegie cyclotron the dependence of the asymmetry on the relative orientation of the axis of the analyzer and the centroid of the incident beam was studied in detail by using a pencil beam of polarized protons. The beam momentum was varied by degrading the protons so that the polarization was constant. The results of these meas-

urements may be accurately summarized by an empirical function $a_j(y,\theta,p)$ which has the following form:

$$a_j(y,\theta,p) = A_0^j(p) + A_1^j(p)y + A_2^j(p)\theta + A_3^j(p)y\theta + A_4^j(p)y\theta^2$$
$$+ A_5^j(p)y^2\theta + A_6^j(p)y^2 + A_7^j(p)\theta^2 + A_8^j(p)y^2\theta^2$$
$$+ A_9^j(p)y^3 + A_{10}^j(p)\theta^3 ,$$

where the A_ℓ^j were taken to be quadratic functions of the recoil proton momentum, p

$$A_\ell^j(p) = D_{\ell 1}^j + D_{\ell 2}^j p + D_{\ell 3}^j p^2 .$$

The function a_j has the following meaning: if a 40% polarized proton beam of momentum p enters the analyzer with an orientation specified by y and θ (see Fig. 4), the asymmetry is $a_j(y,\theta,p)$, where j specifies the configuration of the analyzer (i.e., the thickness of the carbon target and lead absorber). The function is the best fit to calibration data points with the arguments in the range y: ±1 in.; θ: ±1°; and p: 0.456 to 0.975 GeV/c. The values of the D coefficients are given in Ref. 12. The behavior of a at p = 0.954 GeV/c (400 MeV) is illustrated in Fig. 5.

From the function $a(y,\theta,p)$, the analyzing powers $A^j(p)$ have been obtained as

$$A^j(p) = a_j(0,0,p)/0.40 .$$

The function $\mathcal{A}_j(y,\Theta,p)$ also contains the information necessary in making corrections to the asymmetries measured in the primary experiment due to the centroid of the recoil beam having values of y and Θ different from zero. From the spark chamber data, the centroid of the recoil beam can be specified in a coordinate system centered on the axis of the analyzer. Suppose for a particular run the beam coordinates are y_c and Θ_c. Then it can be shown that the asymmetry measured during this run, $\epsilon_M^j(y_c,\Theta_c,p)$, is related to the "true asymmetry" $\epsilon_T^j(0,0,p)$ by

$$\epsilon_T^j(0,0,p) = \epsilon_M^j(y_c,\Theta_c,p) - \alpha_j(y_c,\Theta_c,p) + O(\alpha^2) ,$$

where

$$\alpha_j(y_c,\Theta_c,p) = \mathcal{A}_j(y_c,\Theta_c,p) - \mathcal{A}_j(0,0,p)$$

In all cases the terms containing α to powers ≥ 2 were negligible.

Thus, for each experimental data point the average recoil beam trajectory is determined from the spark chamber data and the corresponding measured asymmetry is corrected, using the relations given above, to give the "true asymmetry." These corrections were generally quite small (typically $\bar{\alpha}_j \tilde{=} 0.01$). As corrections from other sources were not required, the final value of the polarization is obtained by dividing the "true asymmetry" with the appropriate analyzing power $A^j(p)$.

B. Errors

The quoted uncertainty in the polarization measurements contains contributions from statistical counting errors, uncertainty in the determination of

the beam centroid, and an estimate of the systematic error due to instrumental biases. The errors quoted do not contain a contribution due to the uncertainty in the polarization of the beam used in the calibration experiment. This uncertainty is estimated to be ±5% of the polarization and affects all of our data in the same way, irrespective of the recoil proton momentum. Careful checks were made to insure that the results contained no significant errors due to asymmetric accidental events, scanning biases, and incident beam polarization.

In computing the statistical counting errors in the asymmetry the appropriate relation is

$$\Delta\epsilon_{stat.} = \pm\sqrt{(1-\epsilon^2)/N}$$

where N = L+R is the total number of protons analyzed by both the left and right telescopes. In typical runs $\Delta\epsilon_{stat.} \approx \pm 0.004$.

The displacement and angle of the centroid of the recoil proton beam relative to the axis of the analyzer were known statistically to within ±0.020 in. and ±0.025°, respectively, for each data point. This results in an uncertainty in ϵ, the asymmetry, of $\Delta\epsilon_{(y,\theta)} \approx \pm 0.006$.

In order to minimize the effect of any instrumental asymmetries in the analyzing telescopes, the telescopes were periodically interchanged by a 180° rotation of the telescope carriage about the recoil beam line. The average of the asymmetry measured in the two supplementary orientations will contain an error of $1/2\ (c\epsilon_o)$, where ϵ_o is the unbiased asymmetry and c is a parameter which expresses the difference in the sensitivity of the two telescopes and

their associated electronics. It is experimentally known that c is $\ll 0.1$. Therefore the maximum error in ϵ is $\lesssim 0.005$. The typical value of this error is expected to be much less.

Throughout the measurements the incident beam intensity was adjusted so that all important accidental rates remained below 2%. To check that the measured asymmetry was not strongly dependent on the accidental rates, data were occasionally taken with accidental rates of ≈10% and compared with the results obtained at ≈0.5%. There existed no statistically significant difference in the results and we conclude that any errors due to asymmetric accidentals are negligible.

To minimize bias in the measurement of the relative position of the beam centroid and axis of the analyzer from the spark chamber film we have measured all frames twice. For the second scanning the film was viewed with emulsion side "up" instead of "down." The difference between the two scans was less than the corresponding statistical errors associated with the centroid parameters. The bias remaining in the average of the results of the two scannings can be neglected.

If the incident proton beam were polarized. it would have been necessary to apply corrections to our data to obtain the polarization parameter. However, the incident polarization has been measured and found to be consistent with zero. In Fig. 6 we illustrate the relative intensity of protons scattered into the analyzer for recoil proton angles of $\pm\theta_2$, assuming the external proton beam becomes polarized in the extraction process by an amount P_1. For the case of the analyzer on the left of the incident beam axis, the final asymmetry is

given by

$$\epsilon_L = (P_2P_3 + P_1P_3)/(1+P_1P_2) ,$$

where $P_2 = P(\theta_2)$ is the polarization parameter for p-p scattering and P_3 is the analyzing power of the analyzer. For the case of the analyzer being on the right of the incident beam axis, the final asymmetry is given by

$$\epsilon_R = (P_2P_3 - P_1P_3)/(1 - P_1P_2).$$

Therefore, an incident beam polarization P_1 causes a difference in the two asymmetries ϵ_L and ϵ_R of an amount $\Delta\epsilon = 2P_1P_3(1-P_2^2)/(1-P_1^2P_2^2)$. Corresponding measurements of ϵ_L and ϵ_R were made for most of the data points. No systematic difference between the two sets of values were found and we conclude that there existed no significant incident beam polarization.

To check the reproducibility of the data we have repeated the measurement of a majority of the data points. In all cases the difference in the results was within the statistical errors.

C. Results

A summary of the final results is given in Table I. Each entry in Table I, in most cases, represents the combined data from two or more separate measurements.

Our data at 0.75 GeV are shown in Fig. 7 along with the data from experiments by Betz, et al.,[13] Cheng,[14] and Ducros, et al.[3] The polarization at

this energy was well established in these previous measurements, and we made measurements at 0.75 GeV only for five cm angles to serve as a general check on the overall accuracy of our technique and to improve our knowledge of the calibration beam polarization. The calibration beam polarization was found to be 0.40 ± 0.02. As is seen in Fig. 7, our results show good agreement with the existing mean curve.

Data from this experiment have been least squares fitted with the empirical function

$$P(T,\theta^*) = \sum_{k=1}^{k=4} \sum_{\ell=1}^{\ell=5} \alpha_{\ell k} T^{\ell-1} \sin\theta^* \, P_{2k-1}(\cos\theta^*) ,$$

where $P(T,\theta^*)$ is the polarization parameter for incident beam energy T and center-of-mass scattering angle θ^*, and $P(\cos\theta^*)$ are Legendre polynomials. The values of the coefficients $\alpha_{\ell k}$ are given in Table II. The smooth curve drawn on the graphs of the data is a plot of the fitting function at the appropriate value of T.

Our results at 1.03 GeV are plotted in Fig. 8. For comparison, the results of the Birmingham group[15] (0.97 GeV) and the Saclay group[3] (1.03 GeV) are also presented. It is seen that all results near this energy are generally consistent.

A graph of the data at 1.32 GeV is exhibited in Fig. 9. The maximum in the fitting function occurs at approximately 40° in the center-of-mass system and has the value of ≈ 0.41.

The results at 1.63 GeV are presented in Fig. 10, together with the results of Grannis, et al.[1] and Bareyre, et al.[2] From this graph, the discrep-

ancy between the results of the two latter experiments is apparent. Our results indicate, as do those of Bareyre, et al., that $\partial P/\partial\theta_{cm}$ is positive in the region of $\theta_{cm} = 30°$.

The results at 2.24 GeV are presented in Fig. 11. The maximum in the fitting function occurs at approximately 32° in the center-of-mass system. The trend of smaller polarization for higher energies continues to be true here.

A graph of our results at 2.84 GeV is exhibited in Fig. 12 together with the results of the Chamberlain group.[1] The agreement here is good, though our values are generally somewhat lower.

In Fig. 13 a plot is shown of the maximum polarization vs. incident beam energy for the range of energies 0.2 to 6.0 GeV.

V. DISCUSSION

Our data indicate that in the energy region 0.75 to 2.84 GeV the polarization in elastic proton-proton scattering varies smoothly with both energy and angle. We note that the polarization becomes very small in the angular region 60° to 70° cm at 1.32, 1.63, and 2.24 GeV. At present this behavior is not theoretically understood. From 1.03 to 2.84 GeV, the maximum in the fitting function occurs at successively smaller center-of-mass scattering angles.

The peak in the maximum polarization occurs at the incident beam energy of $\approx$ 700 MeV and is quite prominent. It is interesting to note that at approximately this energy the total proton-proton cross section is approaching a relative maximum, presumably due to single pion production.

The results from this experiment have been analyzed in terms of two specific predictions developed in the framework of the Regge theory as discussed in Section II. The predictions are that, for fixed small four-momentum transfer, the polarization should vary as

$$\text{(a)}\quad P(s) = as^{b} \qquad \text{(Ref. 9)}$$

$$\text{(b)}\quad P(s) = c(\sigma(\bar{p}p)-\sigma(pp))/\sigma(pp) \qquad \text{(Ref. 8)},$$

where a, b, c are constants, s is the invariant mass squared, and $\sigma(pp)$ and $\sigma(\bar{p}p)$ are total cross sections for proton-proton and proton-antiproton scattering. Data from this experiment were fitted to the two above forms at $t = -0.3(\text{GeV}/c)^2$. The values of the parameters used for the curves in Fig. 14 are $a = 5.915$, $b = -1.475$, and $c = 0.425$. It is seen that both predictions (a) and (b) agree remarkably well with the polarization data over the range 0.75 to ≈ 3.5 GeV. At higher energies, however, prediction (a) appears to give the best agreement.

Phase shift calculations for the proton-proton interaction in the GeV region have been recently reported by Hama.[5] In his analysis it is assumed that the scattering amplitude can be separated into contributions from one-pion and one-boson exchange mechanisms and a contribution due to interactions at very small distances ($\ell = 0$ to 3) and which is characterized by phase shifts that remain as free parameters in the analysis. Searches for solutions were limited to the neighborhood of the extrapolated low energy solutions. Hama's solutions are summarized in Table III. The imaginary part of the phase shifts $\eta(\ell)$ are related to the parameters in the table as

$$r(\ell) = \exp\left(-2\eta(\ell)\right), \quad 1 - r^2(\ell) = \alpha \exp\left\{-\left(\frac{\ell-\ell_0}{\gamma}\right)^2\right\},$$

where the coefficient α is determined from inelastic cross-section data.

In Fig. 15 we have reproduced Hama's solutions A and B and compared them with our experimental results at 1.63 GeV [1.7 GeV polarization data from Ref. 2 were employed in the initial analysis]. Our measurements in the region $70° < \theta_{cms} < 90°$ tend to favor solution A. This corresponds to a peripheral-absorption solution.

In Fig. 16, we have compared the results at 2.84 GeV with the phase shift predictions. At the time of the phase shift calculations, no data existed beyond $\theta_{cms} = 55°$ and nothing could be said about the relative merit of the three solutions. However, our data clearly favor solution A'. This solution also corresponds to peripheral absorption.

ACKNOWLEDGMENTS

The authors wish to thank the Cosmotron staff for their generous help during the setting up and performance of this experiment. Also, we thank the staff of the Carnegie Institute of Technology Nuclear Research Center for their assistance during the performance of the calibration experiment.

We wish to acknowledge the numerous contributions to the experiment by Dr. Martin L. Perl and Dr. Oliver E. Overseth. It is a pleasure to thank Messrs. David Pellett, Smith Powell, Billy Loo, Ronald Seefred, and Orman Haas for their help in setting up and running the experiment.

REFERENCES

1. P. Grannis, J. Arens, F. Betz, O. Chamberlain, B. Dieterle, G. Schultz, G. Shapiro, H. Steiner, L. van Rossum, and D. Weldon, Phys. Rev. 148, 1297 (1966).

2. P. Bareyre, J. F. Detoeuf, L. W. Smith, R. D. Tripp, and L. van Rossum, Nuovo Cimento 20, 1049 (1961).

3. Y. Ducros, A. de Lesquen, J. Movchet, J. C. Raoul, L. van Rossum, J. Deregel, J. M. Fontaine, A. Boucherie, and J. F. Mougel, submitted to the Oxford International Conference on Elementary Particles, Oxford University, England, 1965.

   G. Cozzika, Y. Ducros, A. de Lesquen, J. Movchet, J. C. Raoul, L. van Rossum, J. Deregel, and J. M. Fontaine, submitted to XIII International Conference on High-Energy Physics, University of California, Berkeley, California, 1966.

4. Michael J. Longo, Homer A. Neal, and Oliver E. Overseth, Phys. Rev. Letters 16, 536 (1966).

5. Y. Hama, Prog. Theor. Phys. 35, 261 (1966).

6. L. Wolfenstein and J. Ashkin, Phys. Rev. 85, 947 (1952).

7. S. C. Wright, Phys. Rev. 99, 996 (1955).

8. Y. Hara, Prog. Theor. Phys. 28, 1048 (1962).

9. I. J. Muzinich, Phys. Rev. Letters 9, 475 (1962).

10. M. Jacob and G. C. Wick, Ann. Phys. 7, 404 (1959).

11. M. L. Goldberger, M. T. Grisaru, S. W. MacDowell, and D. Y. Wong, Phys. Rev. 120, 2250 (1960).

12. Homer A. Neal, University of Michigan Report 03106-23-T, 1966 (Thesis, unpublished).

13. F. Betz, J. Arens, O. Chamberlain, H. Dost, P. Grannis, M. Hansroul, L. Holloway, C. Schultz, and G. Shapiro, Phys. Rev. 148, 1289 (1966).

14. David Cheng, Lawrence Radiation Laboratory Report UCRL 11926, 1965 (Thesis, unpublished).

15. R. J. Homer, W. K. MacFarlane, A. W. O'Dell, E. J. Sacharidis, and G. H. Eaton, Nuovo Cimento 23, 690 (1962).

16. M. Borghini, G. Coignet, L. Dick, K. Kuroda, L. di Lella, P. C. Macq, A. Michalowicz, and J. C. Olivier, CERN preprint, November 1966.

FOOTNOTES

*Work supported by the U. S. Office of Naval Research, Contract Nonr-1224(23).

†*National Science Foundation Postdoctoral Fellow at CERN, Geneva.

Permanent address: Department of Physics, Indiana University, Bloomington, Indiana.

TABLE I

POLARIZATION PARAMETER IN ELASTIC PROTON-PROTON SCATTERING

Incident Proton Energy	θ_{cm} (deg)	P	ΔP
	43.85	0.541	0.075
	47.19	0.513	0.044
0.75 GeV	53.25	0.530	0.029
	63.98	0.470	0.067
	86.29	0.097	0.078
	39.88	0.419	0.031
	42.47	0.464	0.040
	53.60	0.481	0.023
	57.81	0.417	0.038
1.03 GeV	61.62	0.325	0.033
	65.32	0.258	0.073
	68.52	0.245	0.033
	71.37	0.265	0.037
	77.25	0.095	0.029
	88.25	-0.021	0.034

TABLE I (Continued)

Incident Proton Energy	θ_{cm} (deg)	P	ΔP
	32.30	0.361	0.036
	34.77	0.403	0.030
	39.06	0.343	0.045
	46.63	0.407	0.025
	49.77	0.339	0.022
1.32 GeV	53.13	0.266	0.020
	61.21	0.190	0.025
	68.26	0.034	0.030
	74.76	0.062	0.032
	81.81	0.059	0.034
	88.23	0.034	0.029
	28.87	0.228	0.029
	32.80	0.352	0.032
	38.55	0.335	0.025
	44.07	0.369	0.020
1.63 GeV	49.67	0.177	0.040
	56.03	0.151	0.053
	61.91	0.141	0.035
	67.04	0.025	0.028
	73.93	0.025	0.030
	80.57	0.000	0.031

TABLE I (Concluded)

Incident Proton Energy	θ_{cm} (deg)	P	ΔP
	25.32	0.227	0.031
	27.09	0.315	0.026
	30.42	0.252	0.026
	36.08	0.292	0.030
	38.74	0.229	0.052
	40.41	0.205	0.025
	43.45	0.178	0.027
2.24 GeV	47.14	0.182	0.033
	50.65	0.163	0.037
	52.25	0.134	0.036
	54.01	0.147	0.032
	57.04	0.048	0.075
	62.22	0.020	0.041
	69.30	0.093	0.050
	85.24	0.006	0.061
	22.18	0.193	0.026
	23.78	0.188	0.054
	31.65	0.237	0.039
	35.91	0.199	0.057
2.84 GeV	41.37	0.175	0.037
	47.15	0.142	0.071
	60.04	0.115	0.055
	72.72	0.043	0.059

TABLE II

EXPANSION COEFFICIENTS FOR POLARIZATION AS A FUNCTION OF θ^* AND T

	$\alpha_{\ell k}$			
$k \rightarrow$ / $\ell \downarrow$	1	2	3	4
1	4.08 ± 0.64	1.50 ± 0.98	5.9 ± 1.3	2.40 ± 0.95
2	-5.5 ± 1.1	-1.6 ± 1.2	-11.3 ± 2.2	-4.2 ± 1.5
3	2.99 ± 0.60	-0.21 ± 0.88	6.80 ± 0.81	2.57 ± 0.19
4	-0.689 ± 0.037	0.65 ± 0.45	- 1.58 ± 0.42	-0.68 ± 0.35
5	0.056 ± 0.019	-0.152 ± 0.059	0.116 ± 0.075	0.070 ± 0.049

TABLE III

p-p PHASE SHIFTS AT 2.0 AND 2.85 GeV (from Ref. 5)

	2.0 GeV		2.85 GeV		
	Sol. A	Sol. B	Sol. A	Sol. A'	Sol. A''
$\delta(^1S_0)$	-73.3°	-70.0°	- 66.8°	-136.5°	-120.0°
$\delta(^3P_0)$	-62.6°	-54.4°	-168.3°	-143.2°	-176.0°
$\delta(^3P_1)$	-60.8°	-61.2°	- 63.4°	- 30.3°	- 63.3°
$\delta(^3P_2)$	5.1°	- 2.8°	- 16.4°	10.1°	- 15.9°
ϵ_2	16.9°	25.2°	19.0°	30.1°	20.0°
$\delta(^1D_2)$	-27.9°	-19.0°	- 45.5°	44.3°	46.0°
$\delta(^3F_2)$	-31.7°	-63.6°	- 28.8°	0.5°	- 25.6°
$\delta(^3F_3)$	0.0°	- 0.5°	- 6.7°	- 12.8°	- 8.0°
$\delta(^3F_4)$	- 2.3°	0.0°	- 5.7°	4.1°	4.3°
ℓ_0	1.97	0.52	2.20	2.54	2.27
γ	2.83	3.79	3.71	3.10	3.53

FIGURE CAPTIONS

Fig. 1. The experimental arrangement.

Fig. 2. Beam layout.

Fig. 3. Block diagram of electronics. $S_1S_1'S_o\boxed{S_2}$, $S\boxed{U}$, and $S\boxed{T}$ represent accidental events.

Fig. 4. Definition of y and θ.

Fig. 5. Asymmetry parameter at 400 MeV.

Fig. 6. Dependence of the final asymmetry on incident beam polarization. U represents the number of protons with spin "up," and D the number with spin "down."

Fig. 7. Polarization in p-p scattering at 0.75 GeV. Open circles represent data from Ref. 13; open squares, data from Ref. 14; shaded triangles, data from Ref. 3.

Fig. 8. Polarization in p-p scattering at 1.03 GeV. Open squares represent data from Ref. 15; shaded triangles, data from Ref. 3.

Fig. 9. Polarization in p-p scattering at 1.32 GeV.

Fig. 10. Polarization in p-p scattering at 1.63 GeV. Open squares represent data from Ref. 1; open triangles, data from Ref. 2.

Fig. 11. Polarization in p-p scattering at 2.24 GeV.

FIGURE CAPTIONS (Concluded)

Fig. 12. Polarization in p-p scattering at 2.84 GeV. Shaded triangles represent data from Ref. 1.

Fig. 13. Maximum polarization as a function of incident beam kinetic energy. Data from other experiments are cited in Ref. 1.

Fig. 14. Predictions of the Regge pole theory. The dashed line represents a smooth interpolation between points calculated from $P = 0.425\left[\sigma(\bar{p}p) - \sigma(pp)\right]/\sigma(pp)$; the solid curve is the fit $P = 5.915(S)^{-1.475}$. The data represented by open squares is taken from Ref. 16. Data from other experiments are cited in Ref. 1.

Fig. 15. Comparison of data at 1.63 GeV with calculated phase shifts. Dark squares represent data from this experiment. Open circles represent data from Ref. 2.

Fig. 16. Comparison of data at 2.84 GeV with calculated phase shifts. Dark squares represent data from this experiment. Open circles represent data from Ref. 1.

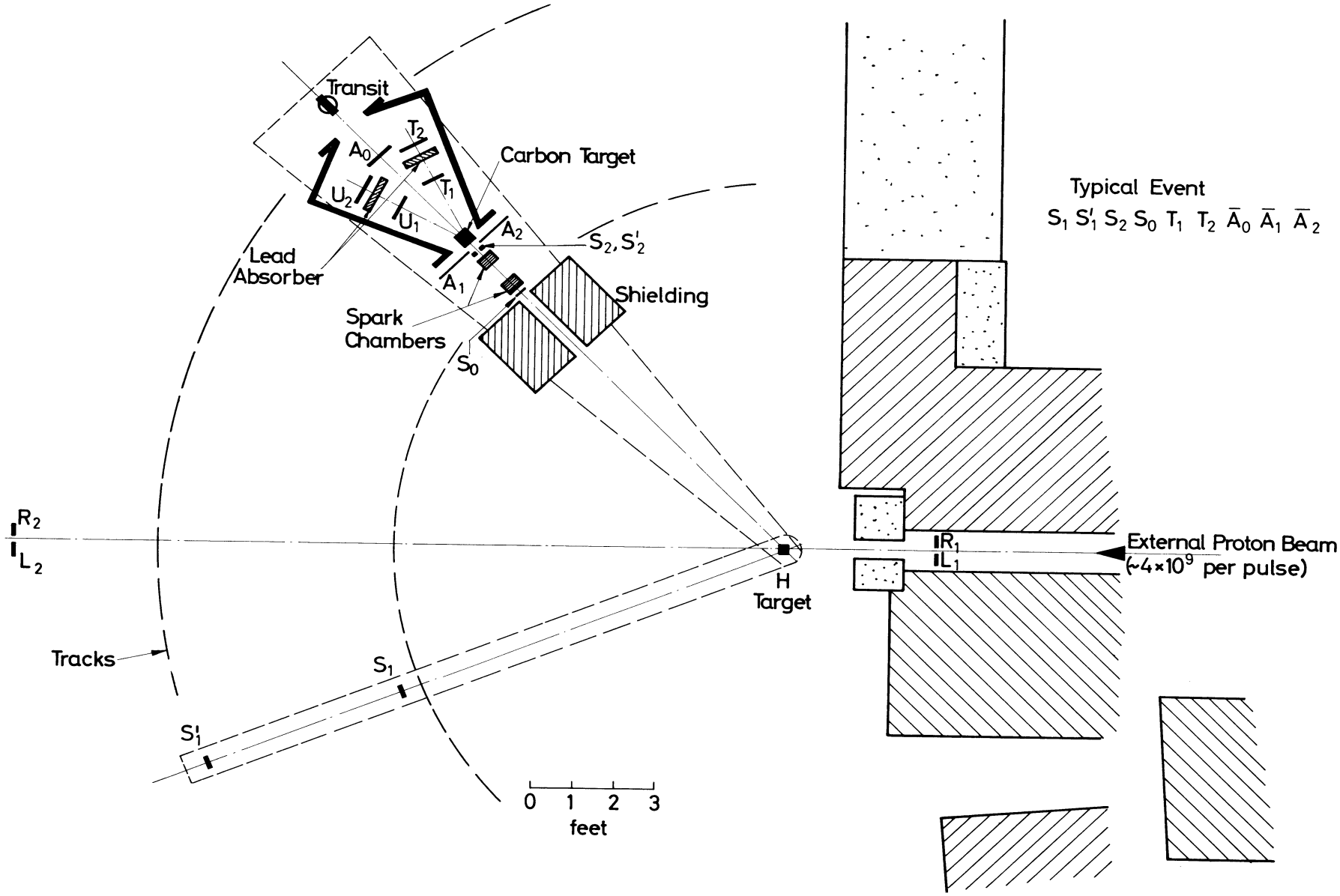
Transit
T_2
A_0
T_1
U_2
U_1
Carbon Target
A_2
S_2, S_2'
Lead Absorber
A_1
Shielding
Spark Chambers
S_0
Typical Event
$S_1\ S_1'\ S_2\ S_0\ T_1\ T_2\ \bar{A}_0\ \bar{A}_1\ \bar{A}_2$
R_2
L_2
R_1
L_1
External Proton Beam
(~4×10^9 per pulse)
H Target
Tracks
S_1
S_1'
0 1 2 3
feet

Fig. 1

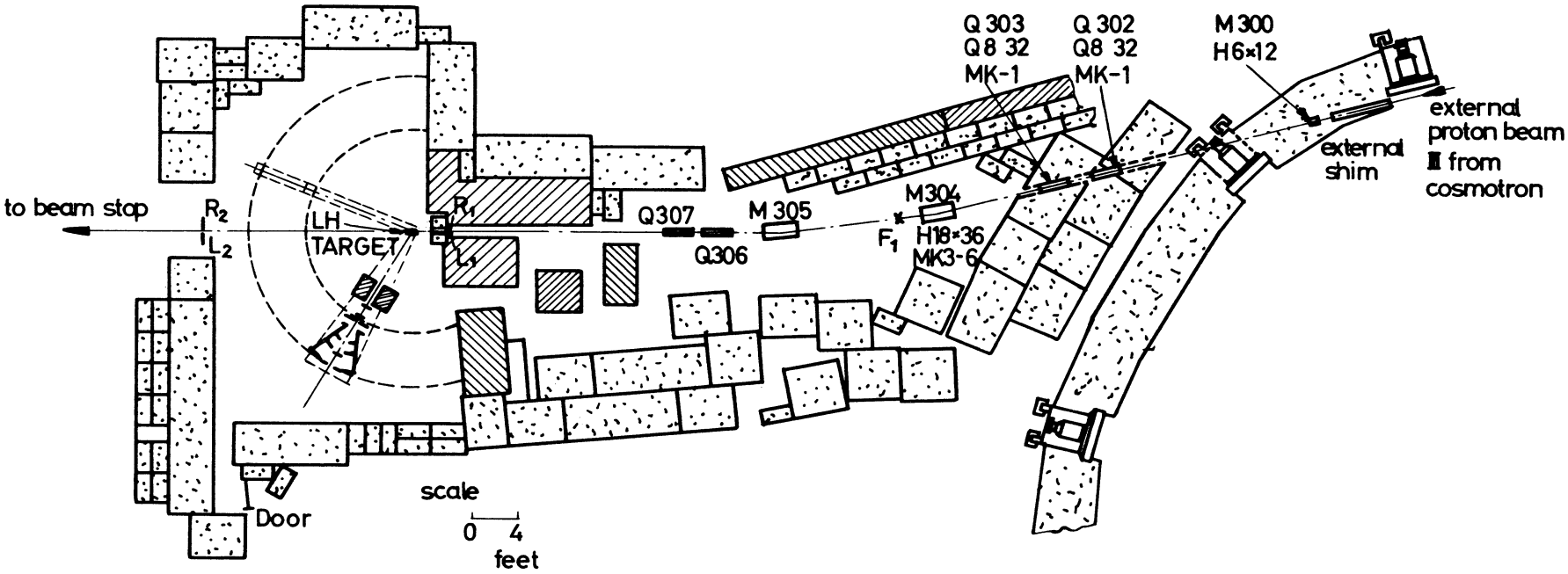
Q 303
Q8 32
MK-1
Q 302
Q8 32
MK-1
M 300
H6×12
external
proton beam
from
cosmotron
external
shim
to beam stop
R2
L2
LH
TARGET
R1
L1
Q307
Q306
M 305
M304
H18×36
MK3-6
F1
Door
scale
0 4
feet

Fig. 2

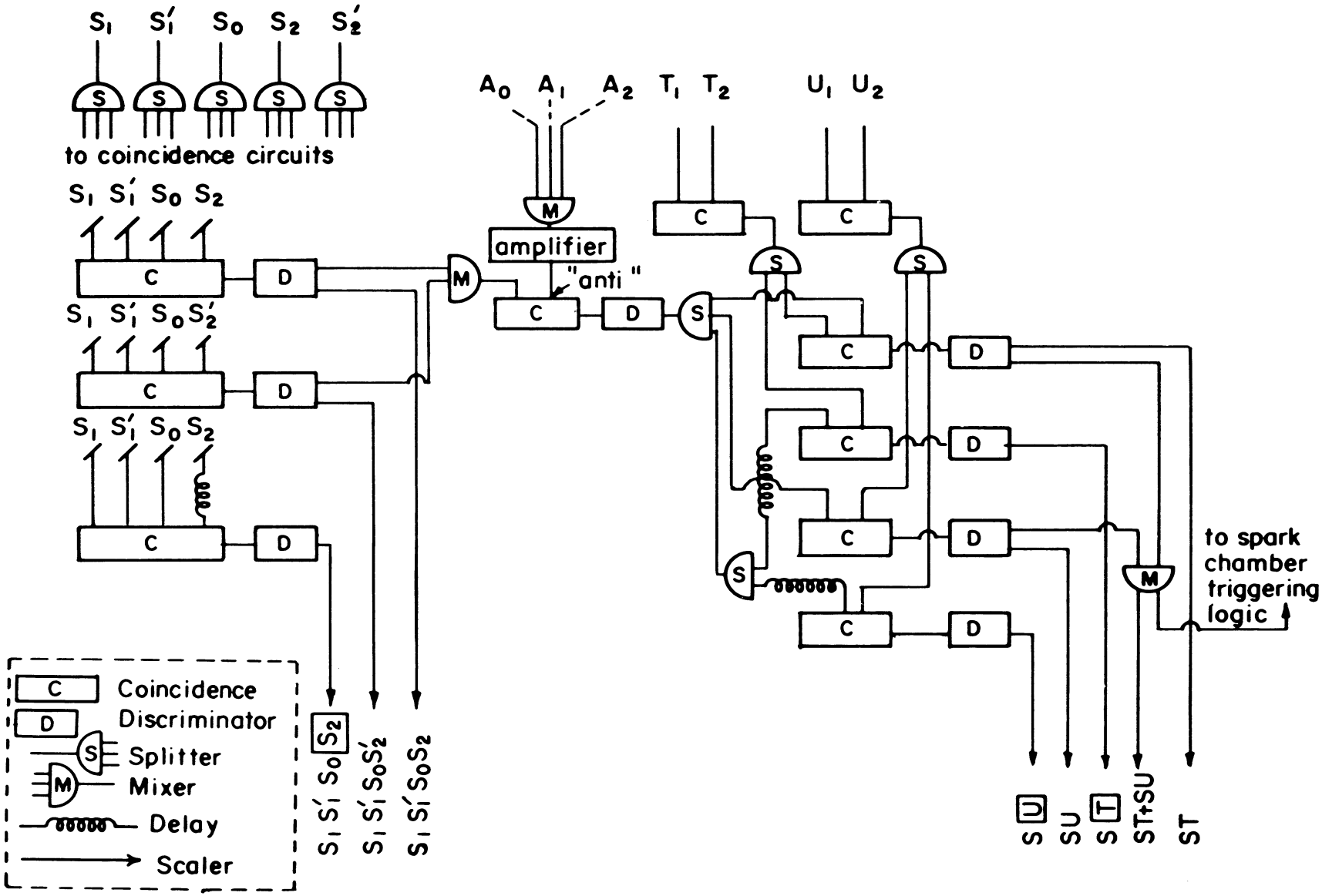
S1 S1' S0 S2 S2'
to coincidence circuits
A0 A1 A2 T1 T2 U1 U2
amplifier
"anti"
to spark chamber triggering logic
Coincidence
Discriminator
Splitter
Mixer
Delay
Scaler
S1 S1' S0 S2
S1 S1' S0 S2'
S1 S1' S0 S2
S1 S1' S0 S2
S1 S1' S0 S2'
S1 S1' S0 S2
S U
SU
S T
ST+SU
ST

Fig. 3

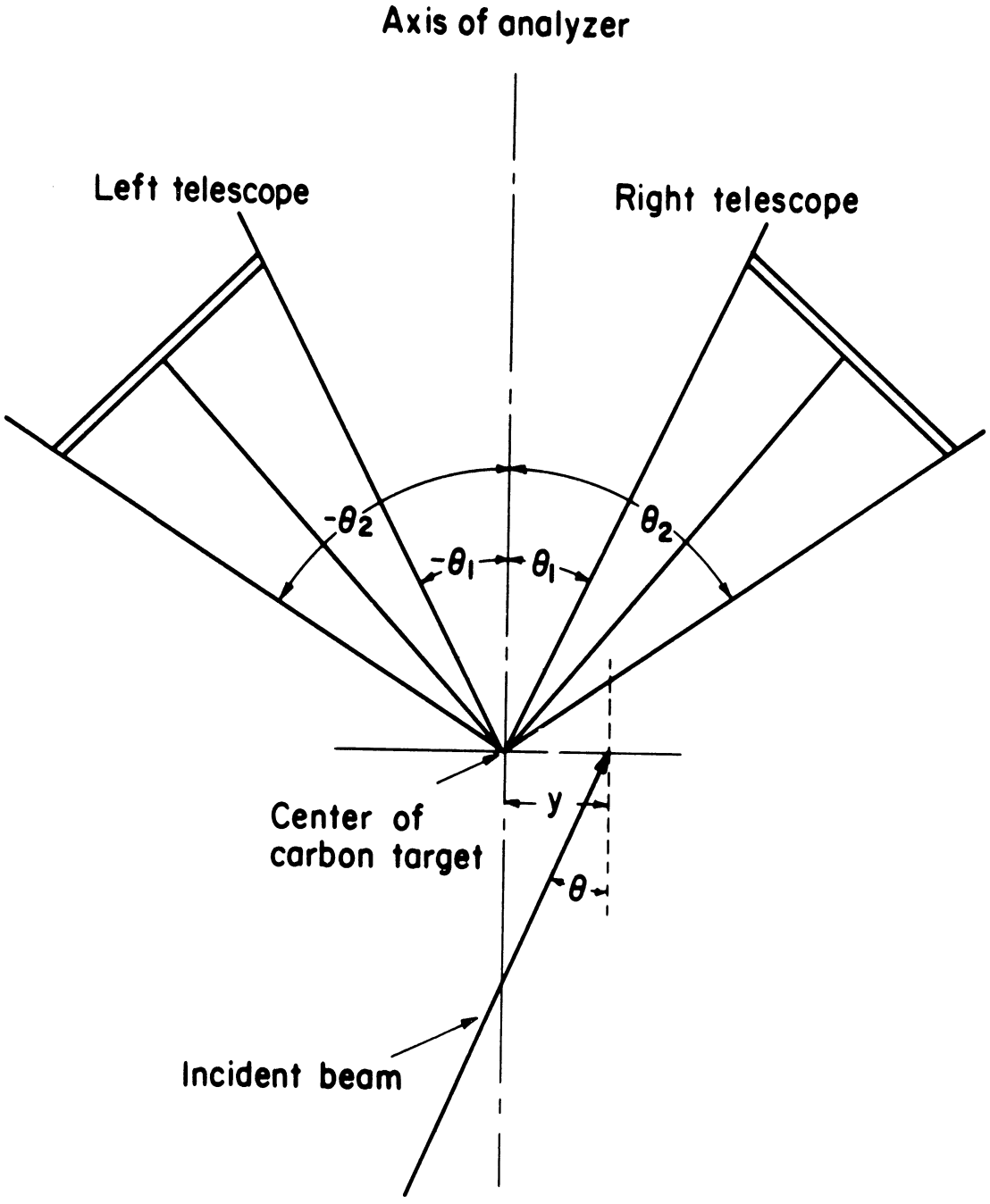
Axis of analyzer
Left telescope
Right telescope
$-\theta_2$
$-\theta_1$
θ_1
θ_2
Center of carbon target
y
θ
Incident beam

Fig. 4

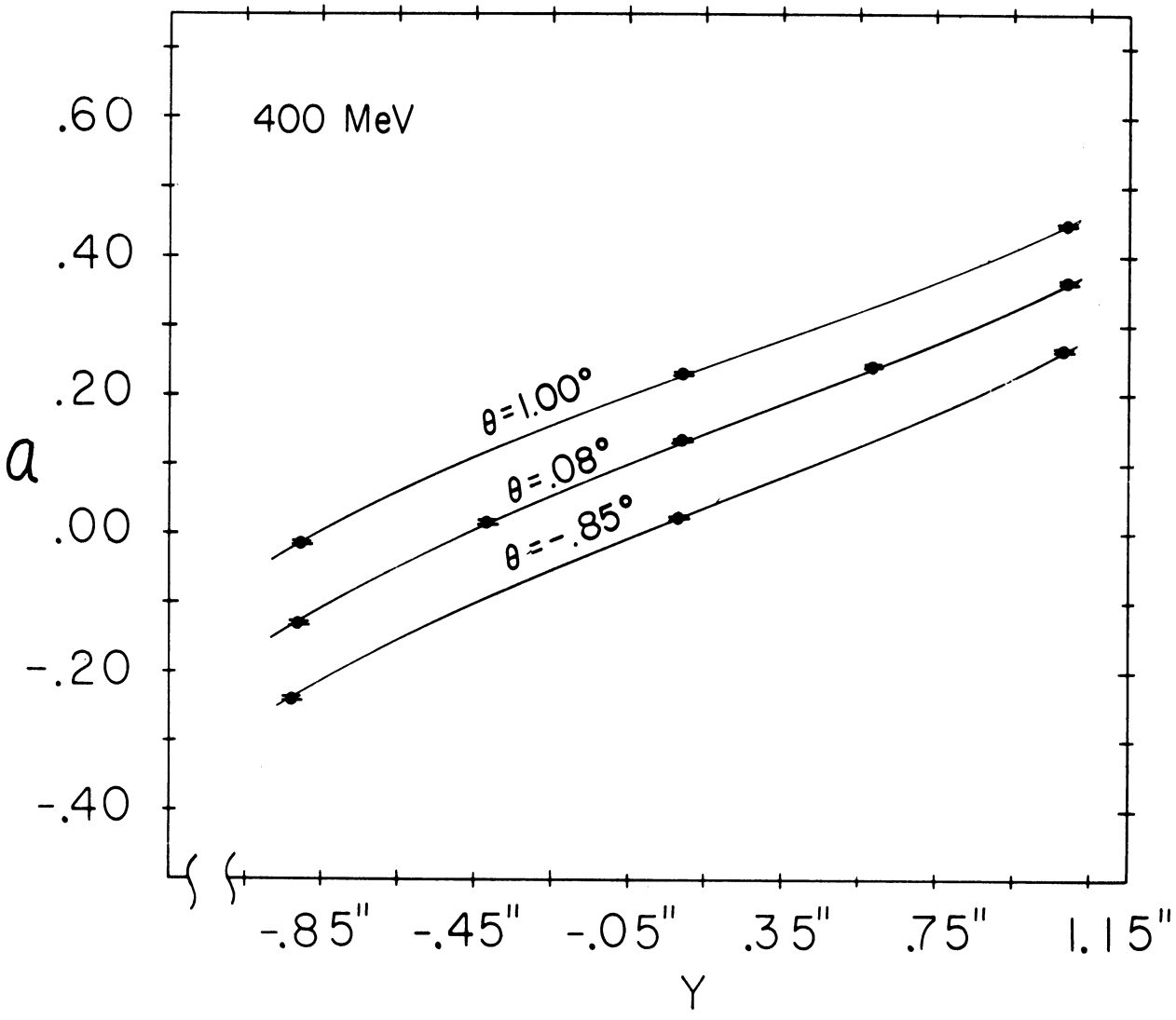

Fig. 5

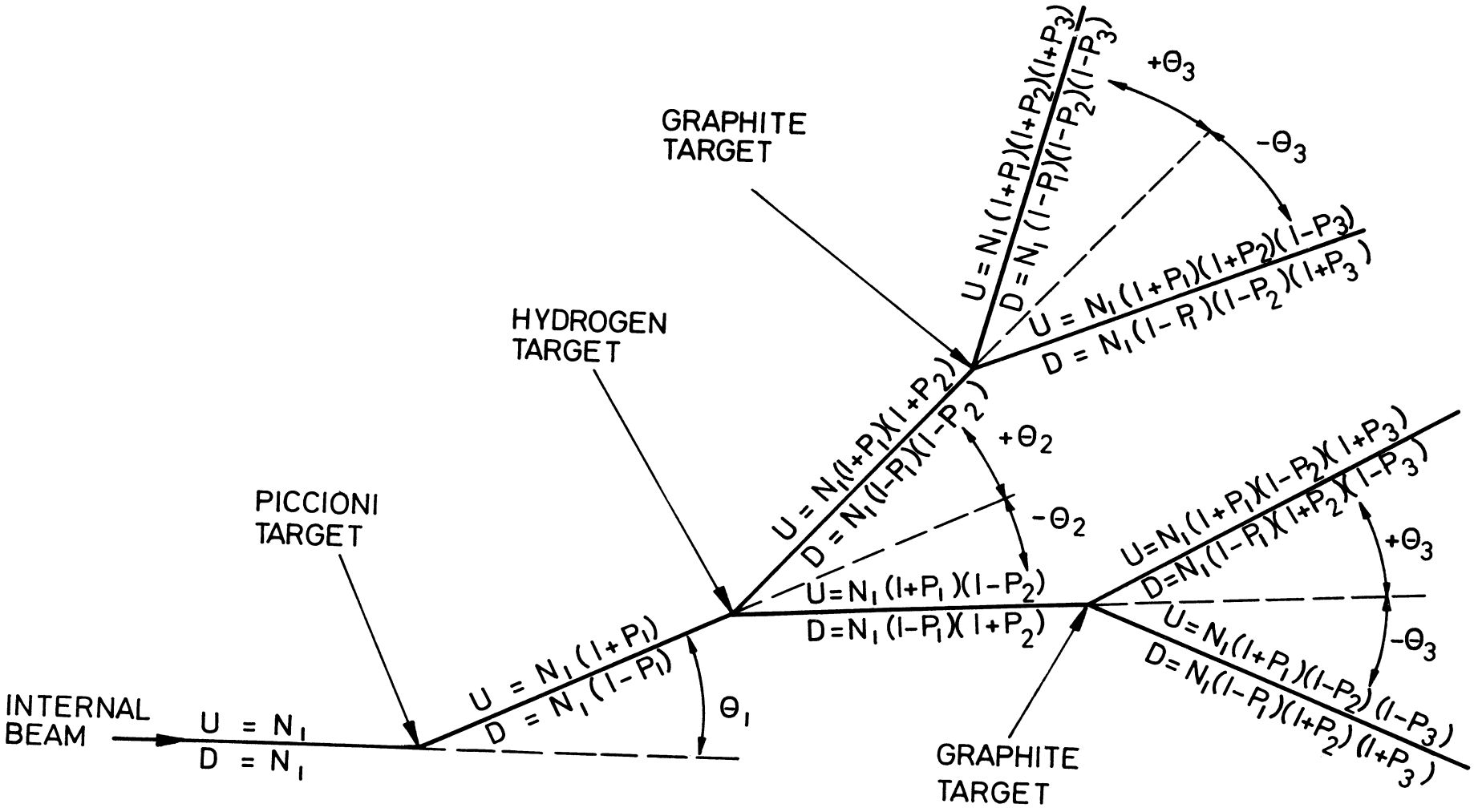
GRAPHITE TARGET
HYDROGEN TARGET
PICCIONI TARGET
INTERNAL BEAM
U = N1
D = N1
U = N1 (1+P1)
D = N1 (1-P1)
θ1
U = N1 (1+P1)(1+P2)
D = N1 (1-P1)(1+P2)
+θ2
-θ2
U = N1 (1+P1)(1-P2)
D = N1 (1-P1)(1+P2)
U = N1 (1+P1)(1+P2)(1+P3)
D = N1 (1-P1)(1-P2)(1-P3)
+θ3
-θ3
U = N1 (1+P1)(1+P2)(1-P3)
D = N1 (1-P1)(1-P2)(1+P3)
U = N1 (1+P1)(1-P2)(1+P3)
D = N1 (1-P1)(1+P2)(1-P3)
U = N1 (1+P1)(1-P2)(1-P3)
D = N1 (1-P1)(1+P2)(1+P3)
GRAPHITE TARGET

Fig. 6

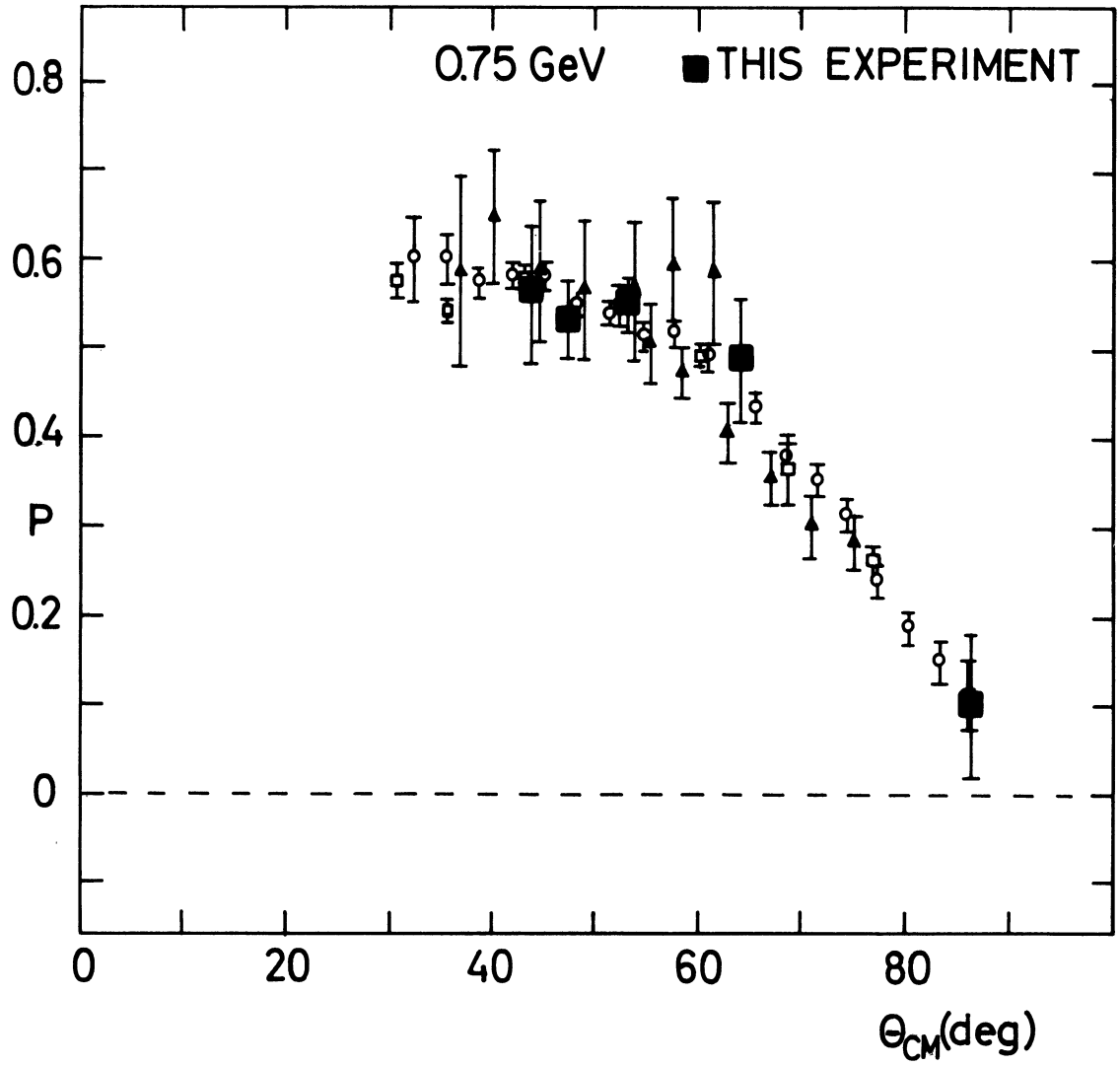

Fig. 7

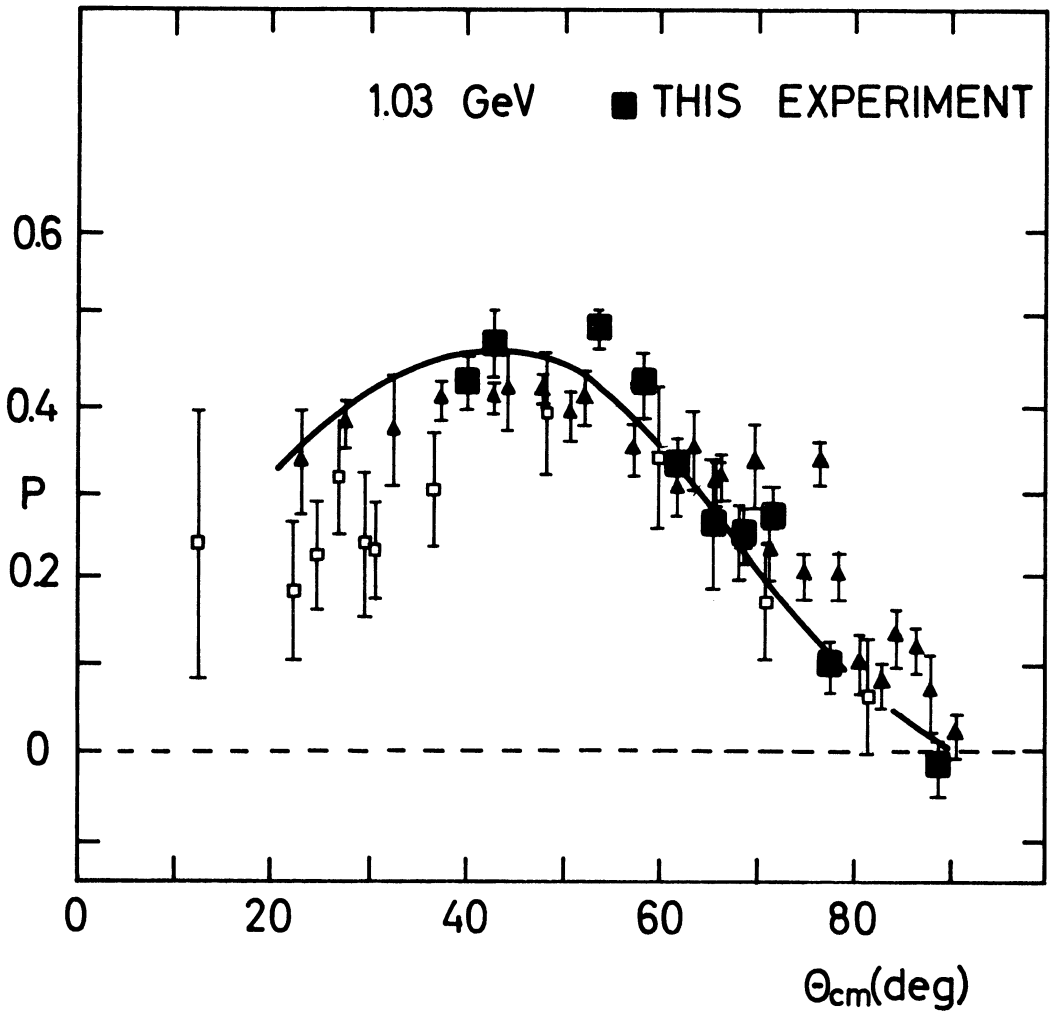

Fig. 8

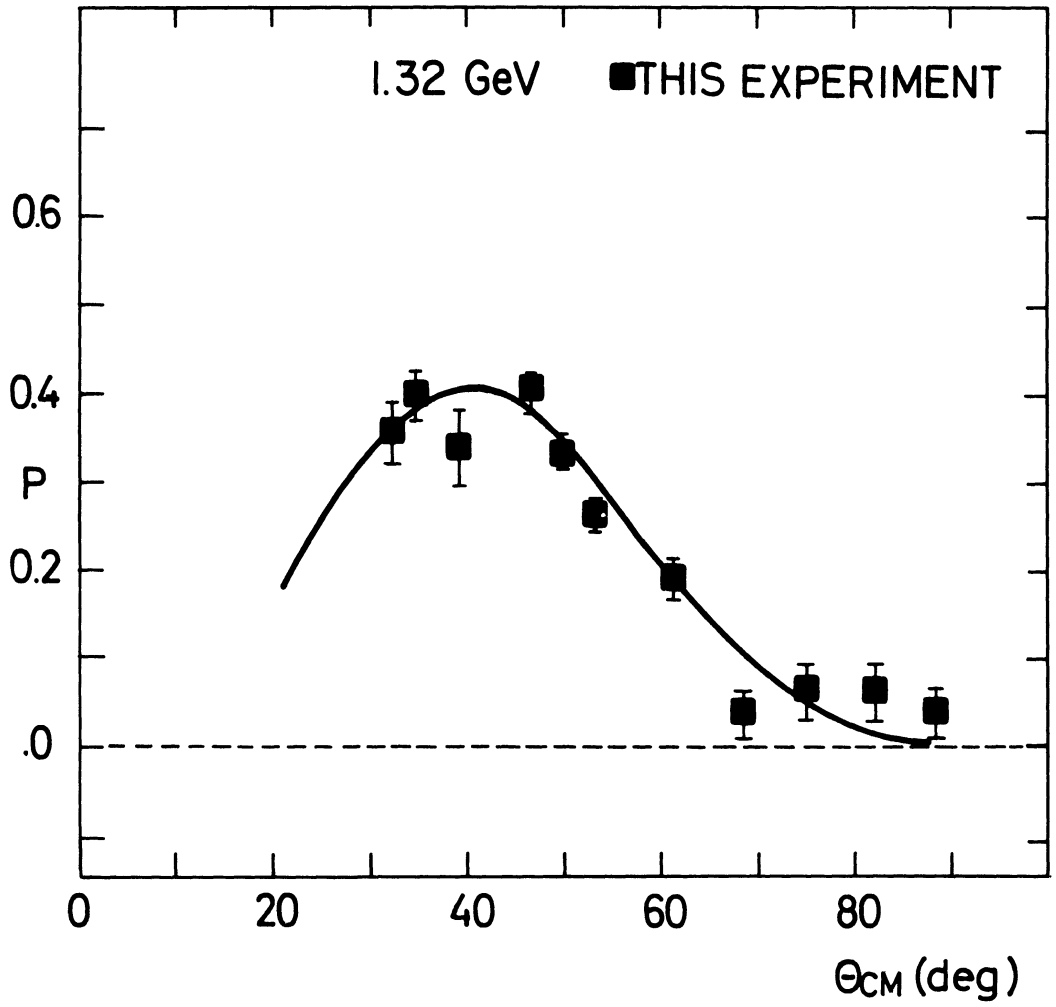

Fig. 9

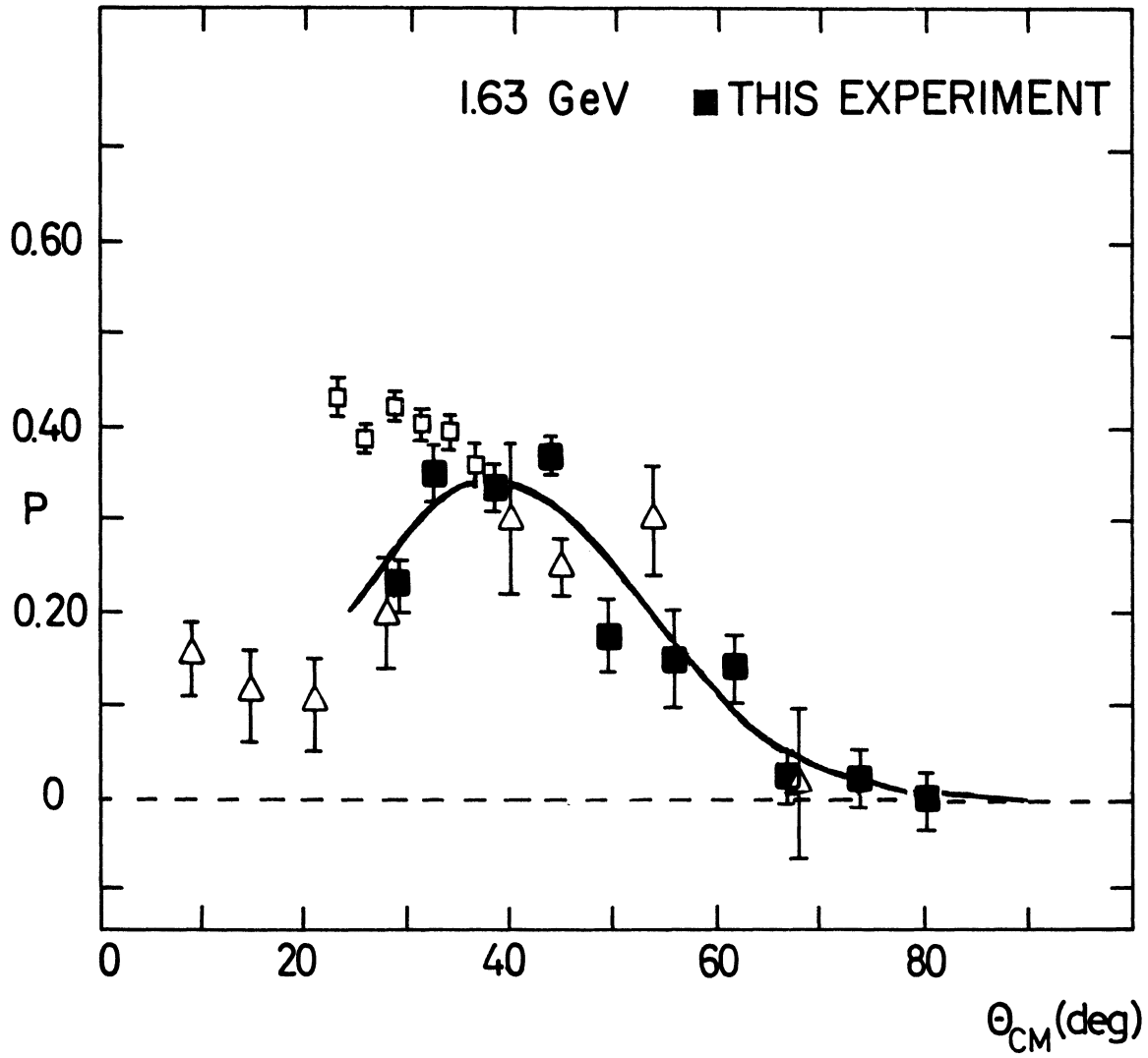
1.63 GeV
THIS EXPERIMENT
0.60
0.40
P
0.20
0
0
20
40
60
80
Θ_{CM}(deg)

Fig. 10

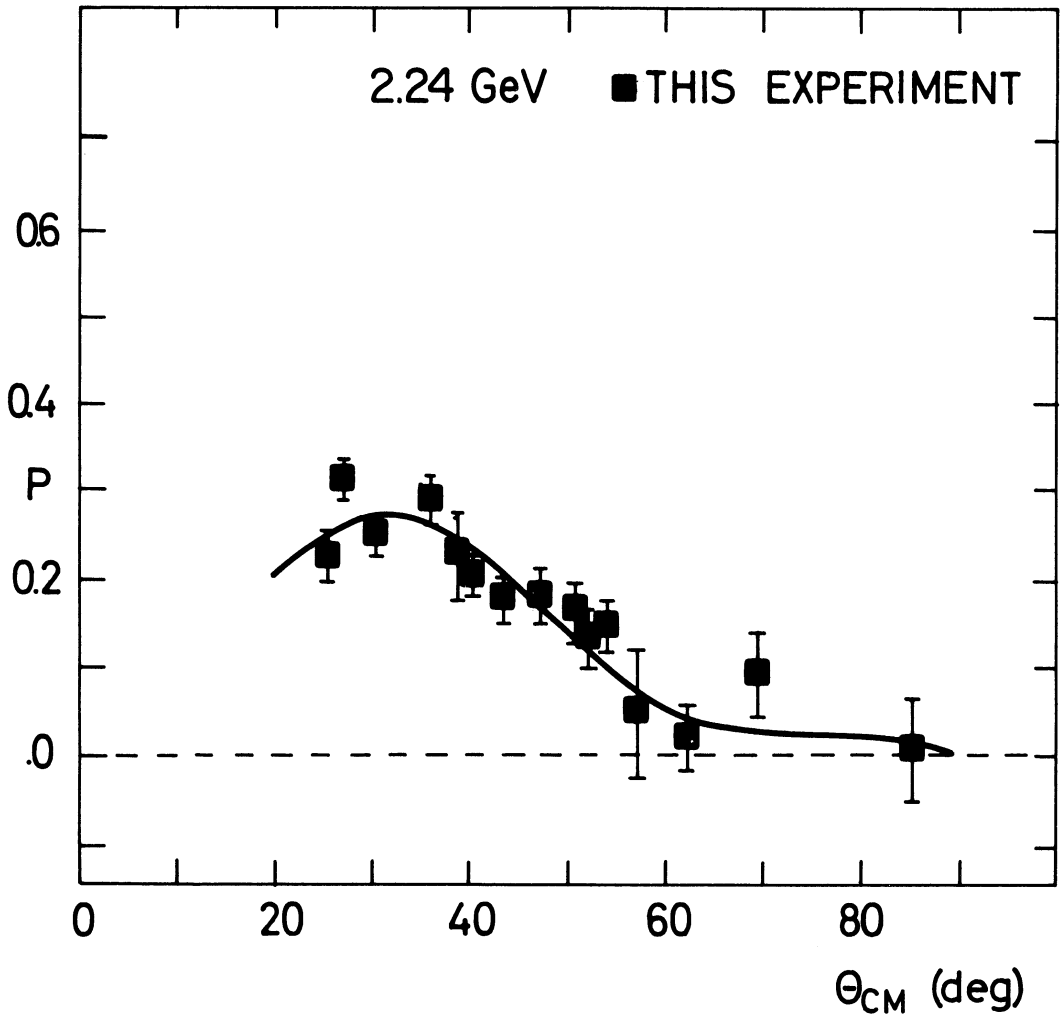

Fig. 11

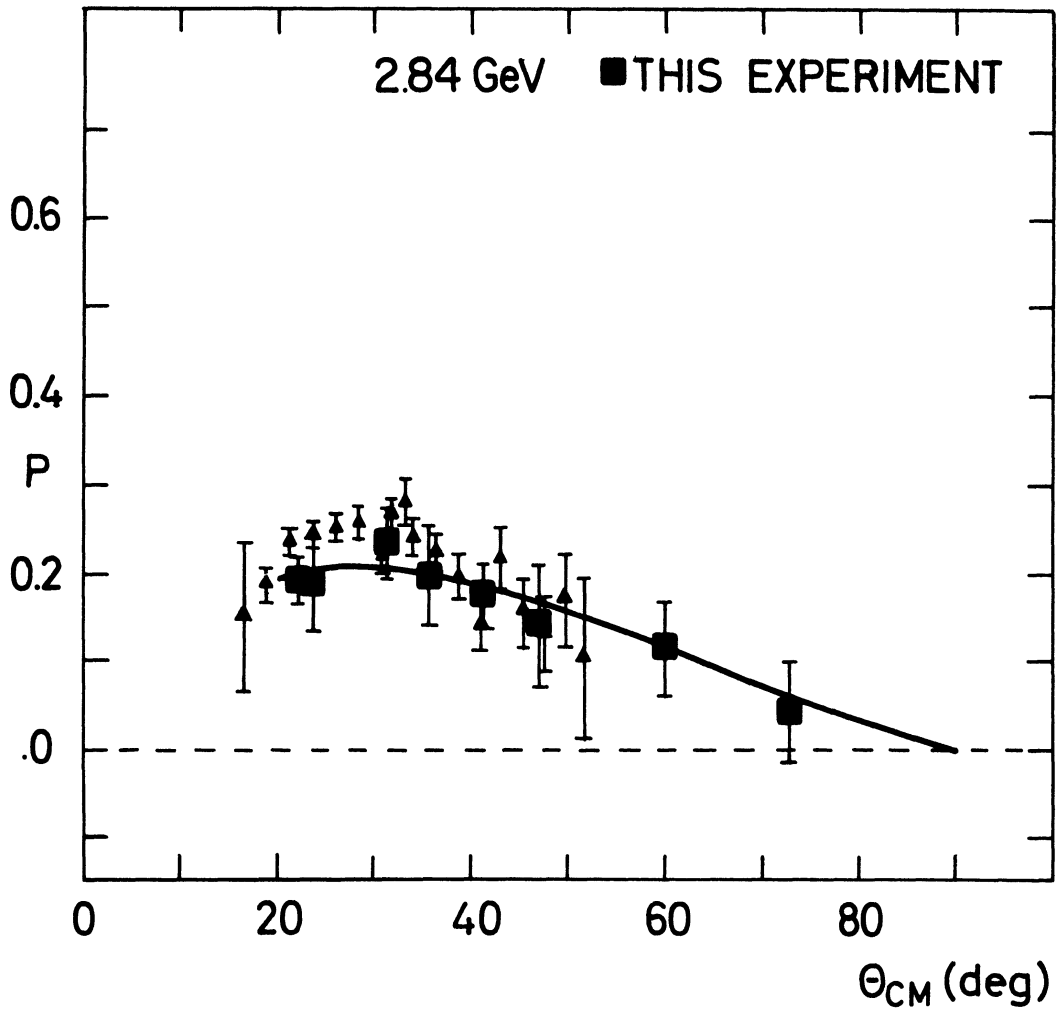

Fig. 12

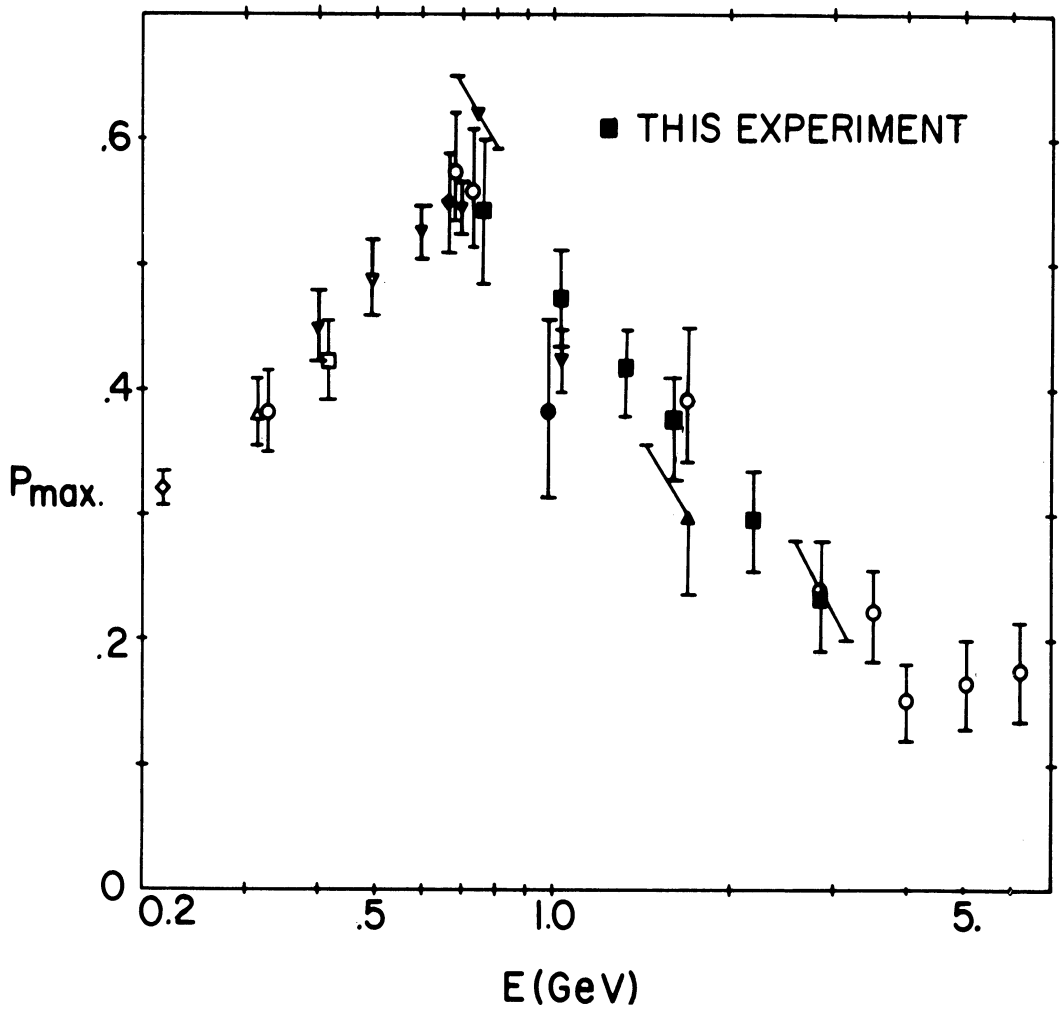

Fig. 13

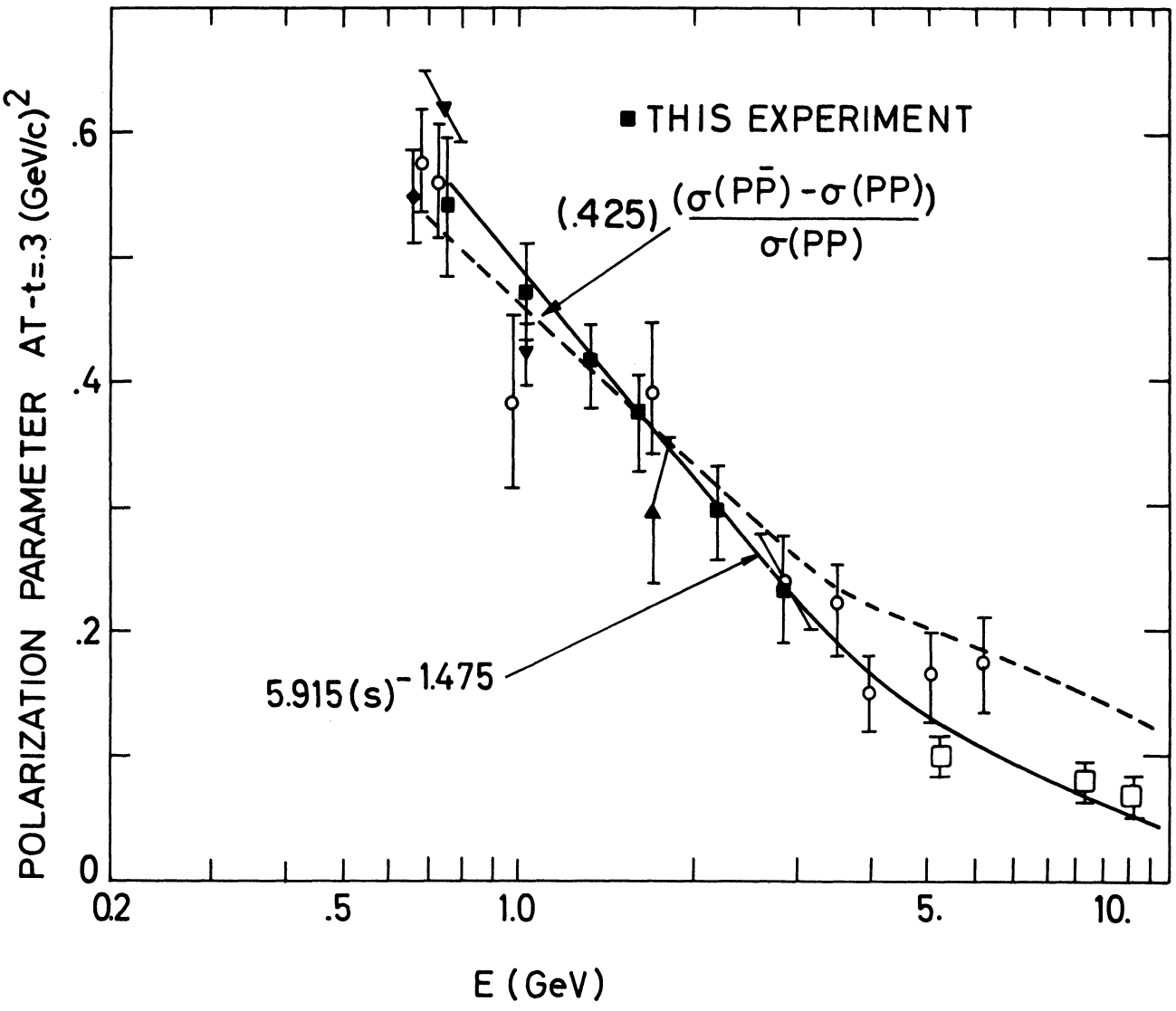
POLARIZATION PARAMETER AT -t=.3 (GeV/c)^2
.6
.4
.2
0
0.2
.5
1.0
5.
10.
E (GeV)
■ THIS EXPERIMENT
(.425) $\frac{(\sigma(P\bar{P}) - \sigma(PP))}{\sigma(PP)}$
5.915 (s)$^{-1.475}$

Fig. 14

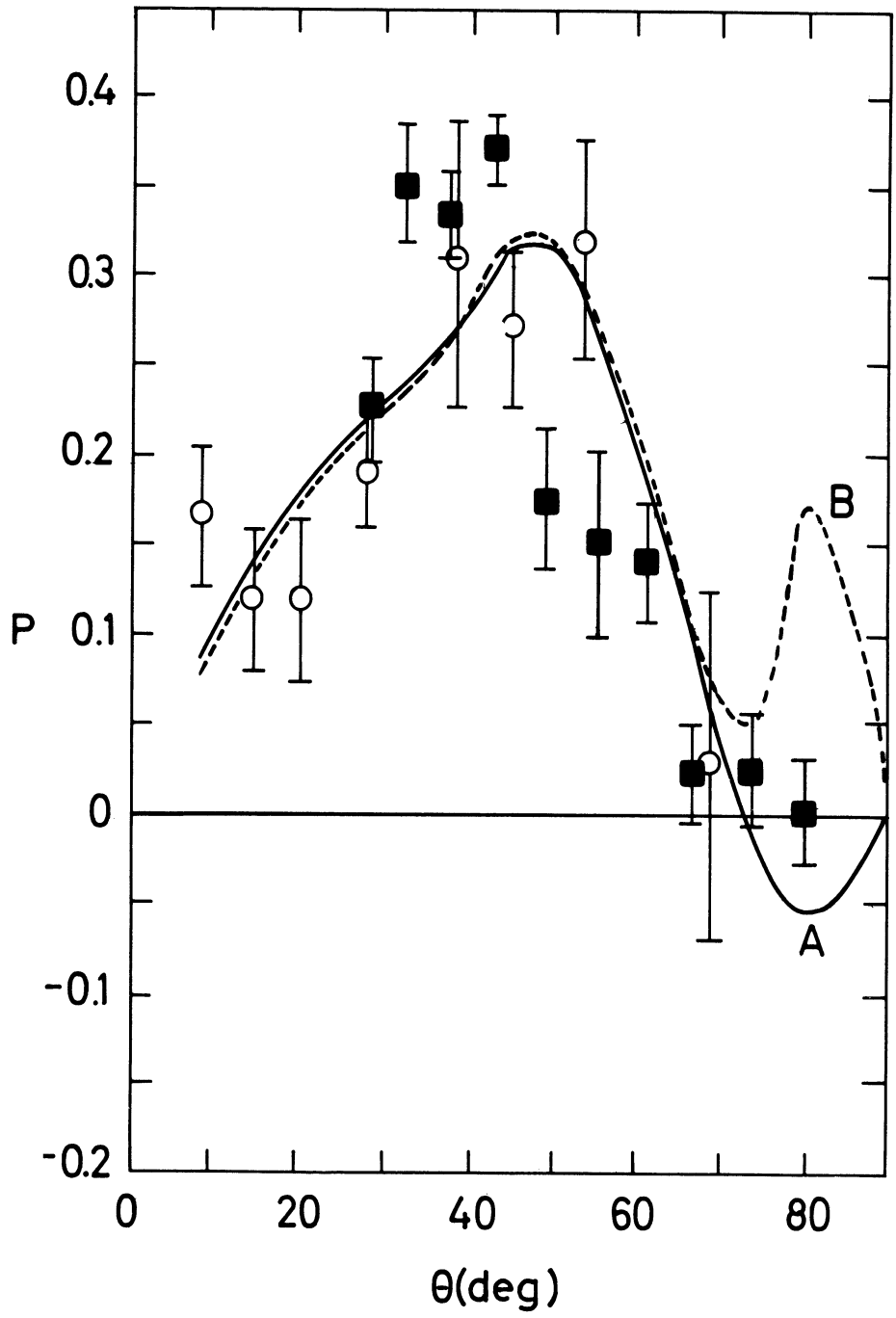

Fig. 15

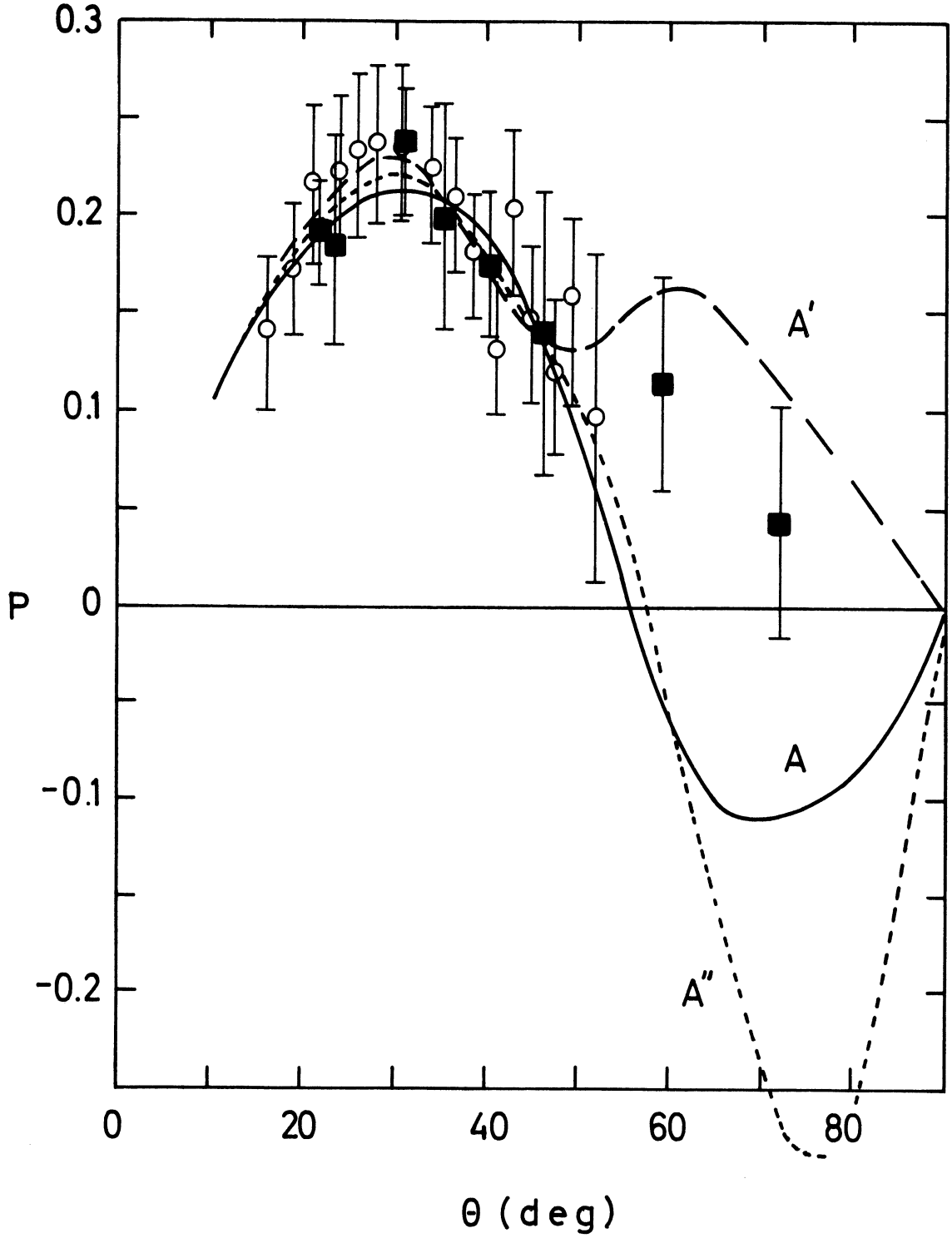

Fig. 16

Unclassified

Security Classification

DOCUMENT CONTROL DATA - R&D

(Security classification of title, body of abstract and indexing annotation must be entered when the overall report is classified)

1. ORIGINATING ACTIVITY (Corporate author)	2a. REPORT SECURITY CLASSIFICATION
The University of Michigan Department of Physics Ann Arbor, Michigan	Unclassified 2b. GROUP

3. REPORT TITLE

POLARIZATION PARAMETER IN ELASTIC PROTON-PROTON SCATTERING FROM 0.75 TO 2.84 GeV

4. DESCRIPTIVE NOTES (Type of report and inclusive dates)

Technical Report

5. AUTHOR(S) (Last name, first name, initial)

Neal, Homer A.
Longo, Michael J.

6. REPORT DATE	7a. TOTAL NO. OF PAGES	7b. NO. OF REFS
March 1967	31	14

8a. CONTRACT OR GRANT NO.	9a. ORIGINATOR'S REPORT NUMBER(S)
Nonr-1224(23) b. PROJECT NO. NR-022-274 c. d.	03106-27-T 9b. OTHER REPORT NO(S) (Any other numbers that may be assigned this report) Technical Report No. 27

10. AVAILABILITY/LIMITATION NOTICES

Distribution of this document is unlimited.

11. SUPPLEMENTARY NOTES	12. SPONSORING MILITARY ACTIVITY
	Department of the Navy Office of Naval Research Washington, D. C.

13. ABSTRACT The polarization parameter in elastic proton-proton scattering has been measured at 0.75, 1.03, 1.32, 2.24, and 2.84 GeV by employing a double-scattering technique. An external proton beam from the Brookhaven Cosmotron was focused on a three-inch long liquid hydrogen target and the elastic recoil and scattered protons were detected in coincidence by scintillation counters. The polarization of the recoil beam was determined from the azimuthal asymmetry exhibited in its scattering from a carbon target. This asymmetry was measured by a pair of scintillation counter telescopes which symmetrically viewed the carbon target. The analyzing power of this system was previously determined in an independent calibration experiment employing a 40% polarized proton beam at the Carnegie Institute of Technology synchro-cyclotron. False asymmetries were cancelled to a high order by periodically rotating the analyzer 180° about the recoil beam line. Spark chambers were utilized to obtain the spatial distribution of the beam as it entered the analyzer; this information allowed an accurate determination of the corrections necessary to compensate for any misalignment of the axis of the analyzer relative to the incident beam centroid. Values of the polarization parameter as a function of the center-of-mass scattering angle are given for each incident beam energy. The predictions of the Regge theory for polarization in elastic proton-proton scattering and recently published phase shift solutions are compared with the experimental results. Surprisingly good agreement with the Regge predictions is found despite the low energies involved.

DD FORM 1 JAN 64 1473

Unclassified

Security Classification

14. KEY WORDS.	LINK A		LINK B		LINK C	
	ROLE	WT	ROLE	WT	ROLE	WT
Polarization Proton-proton scattering						

INSTRUCTIONS

1. ORIGINATING ACTIVITY: Enter the name and address of the contractor, subcontractor, grantee, Department of Defense activity or other organization *(corporate author)* issuing the report.

2a. REPORT SECURITY CLASSIFICATION: Enter the overall security classification of the report. Indicate whether "Restricted Data" is included. Marking is to be in accordance with appropriate security regulations.

2b. GROUP: Automatic downgrading is specified in DoD Directive 5200.10 and Armed Forces Industrial Manual. Enter the group number. Also, when applicable, show that optional markings have been used for Group 3 and Group 4 as authorized.

3. REPORT TITLE: Enter the complete report title in all capital letters. Titles in all cases should be unclassified. If a meaningful title cannot be selected without classification, show title classification in all capitals in parenthesis immediately following the title.

4. DESCRIPTIVE NOTES: If appropriate, enter the type of report, e.g., interim, progress, summary, annual, or final. Give the inclusive dates when a specific reporting period is covered.

5. AUTHOR(S): Enter the name(s) of author(s) as shown on or in the report. Enter last name, first name, middle initial. If military, show rank and branch of service. The name of the principal author is an absolute minimum requirement.

6. REPORT DATE: Enter the date of the report as day, month, year; or month, year. If more than one date appears on the report, use date of publication.

7a. TOTAL NUMBER OF PAGES: The total page count should follow normal pagination procedures, i.e., enter the number of pages containing information.

7b. NUMBER OF REFERENCES: Enter the total number of references cited in the report.

8a. CONTRACT OR GRANT NUMBER: If appropriate, enter the applicable number of the contract or grant under which the report was written.

8b, 8c, & 8d. PROJECT NUMBER: Enter the appropriate military department identification, such as project number, subproject number, system numbers, task number, etc.

9a. ORIGINATOR'S REPORT NUMBER(S): Enter the official report number by which the document will be identified and controlled by the originating activity. This number must be unique to this report.

9b. OTHER REPORT NUMBER(S): If the report has been assigned any other repcrt numbers *(either by the originator or by the sponsor)*, also enter this number(s).

10. AVAILABILITY/LIMITATION NOTICES: Enter any limitations on further dissemination of the report, other than those imposed by security classification, using standard statements such as:

(1) "Qualified requesters may obtain copies of this report from DDC."

(2) "Foreign announcement and dissemination of this report by DDC is not authorized."

(3) "U. S. Government agencies may obtain copies of this report directly from DDC. Other qualified DDC users shall request through _____."

(4) "U. S. military agencies may obtain copies of this report directly from DDC. Other qualified users shall request through _____."

(5) "All distribution of this report is controlled. Qualified DDC users shall request through _____."

If the report has been furnished to the Office of Technical Services, Department of Commerce, for sale to the public, indicate this fact and enter the price, if known.

11. SUPPLEMENTARY NOTES: Use for additional explanatory notes.

12. SPONSORING MILITARY ACTIVITY: Enter the name of the departmental project office or laboratory sponsoring *(paying for)* the research and development. Include address.

13. ABSTRACT: Enter an abstract giving a brief and factual summary of the document indicative of the report, even though it may also appear elsewhere in the body of the technical report. If additional space is required, a continuation sheet shall be attached.

It is highly desirable that the abstract of classified reports be unclassified. Each paragraph of the abstract shall end with an indication of the military security classification of the information in the paragraph, represented as *(TS), (S), (C), or (U)*.

There is no limitation on the length of the abstract. However, the suggested length is from 150 to 225 words.

14. KEY WORDS: Key words are technically meaningful terms or short phrases that characterize a report and may be used as index entries for cataloging the report. Key words must be selected so that no security classification is required. Identifiers, such as equipment model designation, trade name, military project code name, geographic location, may be used as key words but will be followed by an indication of technical context. The assignment of links, rules, and weights is optional.